

Fatigue of composite pipe joint under axial tension

Ł. Figiel¹ and M. Kamiński²

¹ Institut für Polymerforschung Dresden e.V., GERMANY; email: figiel@ipfdd.de

² Mechanics of Materials Division, Technical University of Łódź, POLAND

ABSTRACT: *The main goal of this paper is presentation of a computational approach to damage evolution within the composite pipe adhesive joint subjected to constant amplitude tension. This approach uses the average shear stress criterion to simulate defect propagation within adhesive layer. The numerical procedures are carried out thanks to the commercial Finite Element Method displacement-based program ANSYS. The prediction of composite pipe joint life is described in terms of defect growth rate and load cycles number. Finally, a relation between the mean cycle load and defect growth rate is obtained from computational studies.*

INTRODUCTION

Composite materials have been extensively used in piping systems for many years as a viable alternative to carbon and stainless steels. Composite pipe has been used in corrosive fluid transport in the petrochemical and pulp industries. Nowadays, composite pipe takes over its importance in the offshore oil and gas industry due to its light-weight and corrosion resistance. Limitations on composite pipe size imposed by manufacturing and transport, requirement of inspection and repair imply composite pipe joints to be inevitable in all piping systems. The continued integrity and long term durability of new composite pipe-works depend, in part, on the integrity of the adhesive bonds for joining the pipe sections as reported in [1]. The composite pipelines used in marine applications exhibit the joints as the weakest link in a composite piping system as reported in [2], what emphasises the importance of composite pipe joints reliability.

In this paper the static fatigue-like behaviour of composite pipe joint under axial tension of constant amplitude is studied computationally. A defect propagation as a function of load cycles is analysed thanks to the Finite Element Method (FEM) displacement-based. The proposed numerical approach makes it possible an estimation of the mean composite pipe joint life in terms of applied mean load.

COMPUTATIONAL MODEL

The deterministic computational model of fatigue-like damage of composite pipe adhesive joint is built upon the following assumptions:

- pipe joint components are linear elastic,
- no initial manufacturing flaws, pre-cracks or other defects exist in the original adhesive layer,
- location of defect nucleation and growth is within adhesive layer and caused by high shear stress intensities,
- fatigue defect propagation is stable.

In the proposed connection (cf. Figure 1), shear stresses along adhesive layer length are not uniform and the stress gradients arise at joint edges from the differential straining of the bonded substrates (composite pipe and coupling) under axial tension.

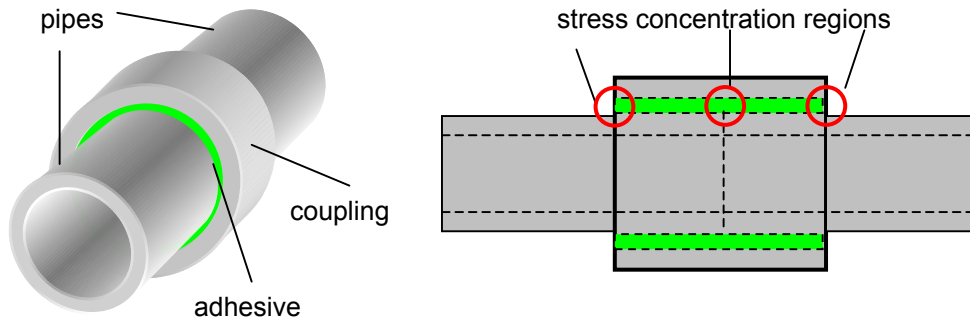


Figure 1: Composite pipe adhesive connection: 3D and 2D views

Defect starts growing along the adhesive layer and uniformly over its circumference, when the average shear stress, $\langle \tau_{ad} \rangle$, resulting from applied tensile load, σ is equal to or greater than the shear static strength, τ_{ad}^u , of adhesive layer

$$\langle \tau_{ad} \rangle = \frac{1}{d} \int_0^d \tau_{ad} dX_A \geq \tau_{ad}^u. \quad (1)$$

The criterion presented by Equation. (1) is called the average stress criterion and first reported by [3]. The distance 'd' is so-called a characteristic length which may stand for the damage accumulated process zone and here it is expressed in terms of the critical mode II fracture mechanics parameter, K_{IIc} , as follows:

$$d = \frac{1}{2\pi} \left(\frac{K_{IIc}}{\tau_{ad}^u} \right)^2. \quad (2)$$

Equation (2) is based on the square-root stress singularity in the front of the sharp crack tip and might not represent the state of stress within tubular adhesive layer in the stress concentration region. However here, this characteristic length serves to estimate an upper bound for the finite element size at the tip of crack-like defect. Then, it is assumed that after defect nucleated, it steadily propagates along the adhesive layer as a main crack-like defect. It leads to average shear stress increase in the stress concentration regions along with the number of cycles N as follows:

$$\langle \tau_{ad}(N) \rangle = \frac{1}{d} \int_0^d \tau_{ad}(N) dX_A \Rightarrow \frac{1}{d} \int_0^d \frac{\tau_{ad}(N)}{1-D(N)} dX_A, \quad (3)$$

where $D(N)$ denotes classical scalar damage variable which may be written in terms of the nucleated and propagating main crack-like defect 'a' as follows:

$$D(N) = \frac{a(N)}{l_a}, \quad (4)$$

The defect propagation terminates under following condition:

$$D(N) = 1 \Leftrightarrow a(N) = l_a. \quad (5)$$

what corresponds to loss of stiffness of all finite elements within adhesive layer.

NUMERICAL SOLUTION

The potential energy of deforming body with damage, D , may be given as follows:

$$\Pi[u_i, D] = U[D] - V[D], \quad (6)$$

where $U[D]$, $V[D]$ denote the strain elastic energy and the external work, respectively.

Then using so-called compatible displacement model of the Finite Element Method (FEM), potential energy may be written as follows:

$$\Pi[u_i, D] = \sum_{e=1}^E \Pi^{(e)}[u_i^{(e)}, D^{(e)}], \quad (7)$$

where the summation extends over a total of E discrete elements taking up the regions Ω_e , respectively, the index 'e' refers to a typical, or e-th, finite

element and $u_i^{(e)}$ are localised displacement functions which vanish everywhere outside of the e-th element [4]. Then, it is assumed that the function $u_i(x_k)$ such that $x_k \in \Omega_e$, can be approximated within each e-th element in terms of shape functions $\phi_{i\xi}^{(e)}(x_k)$ as $u_i^{(e)}(x_k) = \phi_{i\xi}^{(e)}(x_k)q_\xi^{(e)}$ and $\xi = 1, 2, \dots, N^{(e)}$ where $q_\xi^{(e)}$ is the vector of element nodal displacements and $N^{(e)}$ denotes the number of degrees of freedom assumed in the e-th element considered. Under assumption of the linear elastic material behaviour and progressing damage, $\sigma_{ij} = C_{ijkl}(1-D)\epsilon_{kl}$, the total potential energy of the body is written as follows:

$$\Pi[u_i, \Phi] = \sum_{e=1}^E \left[\int_{\Omega_e} \frac{1}{2} \epsilon_{ij}^T (1-D) C_{ijkl} \epsilon_{kl} d\Omega - \int_{\Omega_\sigma} t_i^T u_i d(\partial\Omega) \right], \quad (8)$$

Finally, as a result of the first variation of the potential energy with respect to particular nodal displacement component ($\partial\Pi/\partial q_\alpha$) it is possible to obtain the well-known FEM displacement-based system of algebraic equations to be solved for the unknown nodal displacements as follows:

$$K_{\alpha\beta}(D)q_\beta = Q_\alpha. \quad (9)$$

No energy dissipation due to propagating crack in the sense of Griffith [5] is considered here. That is why the damage propagation is considered as the material volume reduction by a finite element stiffness reduction. Actually, two values are only assigned to the scalar damage variable: $D=0$ or $D=1$ in this work.

NUMERICAL ILLUSTRATION AND DISCUSSION

The purpose of this computational deterministic FEM displacement-based study is to estimate crack-like defect propagation within adhesive layer of the composite pipe joint subjected to tension (cf. Figure 2). The cycle asymmetry ratio is $R=0$ and load amplitude is equal to applied maximum load (σ_{max}). A static fatigue-type load is applied that is why no frequency effect is considered in this work. Each load cycle is divided into two time intervals of 6 months and a time limit corresponds to a cycle in which material fails and is equal to $D(N)=1$. However, the problem considered here is not truly time-dependent and time is a tracking parameter, only.

The axisymmetry of the composite pipe joint geometry implied in a simplification of the computational model. Moreover, half of composite pipe joint in axial direction is considered only due its longitudinal symmetry. Finally, the model analysed via FEM displacement-based commercial program ANSYS [6] is shown in Figure 3. The pipe and coupling component are made up of unidirectional $[0^\circ]$ s E-glass/epoxy composite (50% fibre volume fraction) of material properties taken from [7], and adhesive layer of rubber toughened epoxy found in [8]. All materials properties of composite pipe joint components are tabulated in Table 1.

TABLE 1: Material properties

Property	Rubber toughened epoxy	E-glass/epoxy
Longitudinal modulus [GPa]	3.05	45
Transverse modulus [GPa]	3.05	12
Shear modulus [GPa]	1.13	5.5
Poisson's ratio	0.35	0.28
Shear strength [MPa]	54	70
Tensile strength [MPa]	82	1020
Fracture toughness G_{Ic} [kJ/m^2]	3.4	-
Fracture toughness G_{IIc} [kJ/m^2]	3.55	-

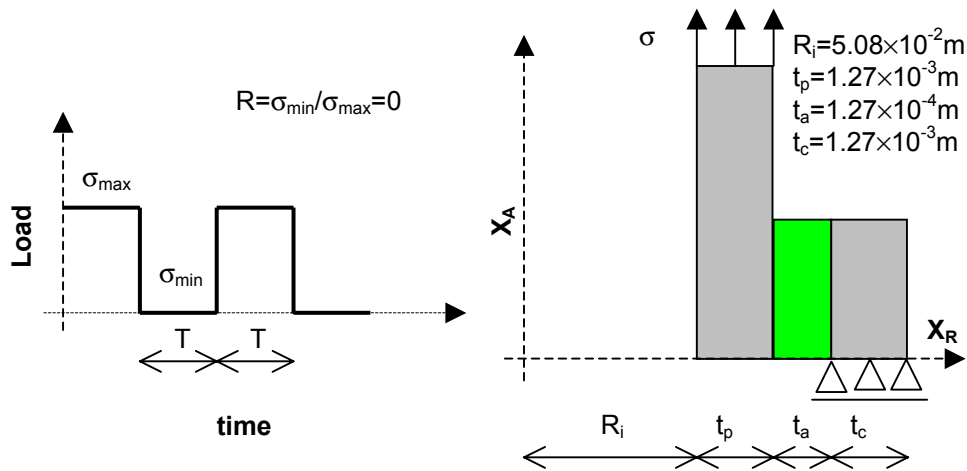


Figure 2: Applied load

Figure 3: Computational model

The axisymmetric FEM analysis was carried out using four node finite elements PLANE42 of three translational degrees of freedom (DOF) (u,v,w) at each node, and of the linear shape functions. The model mesh was designed to be more dense in the region of high stress concentration. In this region the finite element size was equal to the process zone 'd' given by the Equation 2. During loading the average value of shear stress component computed by ANSYS within finite element were compared to the ultimate static shear stress of the adhesive layer. After this value had been exceeded within a finite element, then its stiffness was multiplied by the reduction factor equal to 1×10^{-6} and element was deactivated. An element stiffness deactivation was possible thanks to ANSYS' Birth and Death Element option. The frontal equation solver was used along with the Newton-Raphson iteration technique during the problem solution.

At first, the defect propagation within an adhesive layer, as a function of load cycles, is presented for five different load amplitudes $\sigma_{\max} = 216, 243, 270, 406$ and 540 MPa which correspond to $4 \times, 4.5 \times, 5 \times, 7.5 \times, 10 \times$ of τ_{ad}^u respectively. It was observed that no defect nucleated below load amplitude equal to 216 MPa , that is why this value may estimate the load threshold value for defect propagation within the model considered here. Obviously, it was observed the higher load amplitude the less load cycles required to final failure as shown in Figure 4.

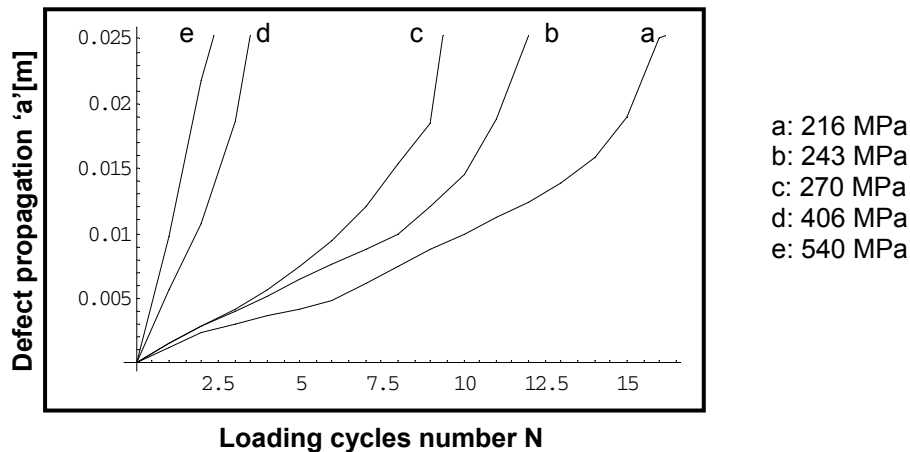


Figure 4: Fatigue defect growth for different load amplitudes

Those results were used to calculate the mean defect propagation rate (mm/cycle) as a function of the applied mean fatigue load through the following formulas:

$$\sigma_m = 0.5(\sigma_{\max} + \sigma_{\min}) \text{ and } (da/dN)_m = \frac{1}{n} \sum_{i=1}^n (da/dN)_i, \quad (10)$$

As a result, the relation between the mean damage propagation rate and the applied mean stress is presented in Figure 5. The logarithmic form was taken in order to obtain coefficients $\alpha=2.3591$ and $\beta=-12.132$ of the function $\ln(a)=\alpha\ln(b)+\beta$. The final relation between the mean defect propagation rate and the applied mean stress is as follows:

$$(da/dN)_m = e^{\left[1 \times 10^{-4}(-121320.0 + 23591.0 \ln(\sigma_m))\right]} \quad (11)$$

Equation (11) makes it possible to estimate the mean defect propagation rate under applied mean fatigue load for the model presented here. Obviously, for the material system with different material properties, it would be necessary to repeat all numerical procedures.

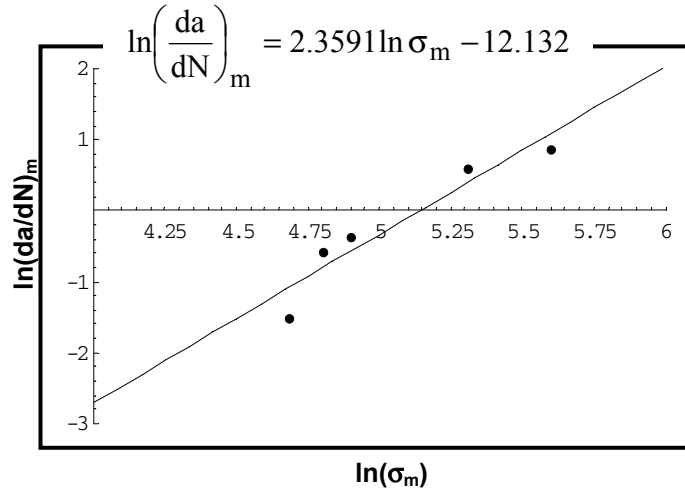


Figure 5: Mean defect growth as a function of applied mean stress

Results presented above were obtained with 2606 finite elements (254 within adhesive layer). Then, next numerical examples have been carried out to estimate the finite elements number effect on the results. It was assumed that finite element number within adhesive layer may only influence results. Thus at first, the vertical mesh division was studied with 400,800,1200,1600,2000,4000 finite elements, respectively. As it was

expected, results became independent along with decreasing finite element size and increasing element number. The vertical element size for which results did not change was equal to $l_e=1\times 10^{-4}$ m.

Presented approach made it possible numerical estimation of fatigue damage evolution within initially undamaged macro-mechanical model subjected to static fatigue tensile load. This approach may especially be convenient to predict life of structures with the high stress concentration regions, where internal stresses even under applied fatigue loading may be high enough to overcome material or component strength. Concluding, on the one hand this computational approach would be more applicable to estimate low-cycle fatigue damage propagation under high load amplitude than to high-cycle of low load amplitude. On the other hand, this approach might serve to simulate a stable defect propagation under increasing static load.

The consideration of fatigue damage zone development in the front of progressing macro-defect can probably improve this model. In such an approach, one should take into account local stiffness decrease in the front of high stress concentration zones along with load cycles number. The study on applicability of the so-called cohesive zone model (CZM) and its FEM displacement-based implementation for meso and macro level fatigue processes modelling is under way.

REFERENCES

1. Knox, E.M., Cowling, M.J., Hashim S.A. (2000) *International Journal of Fatigue* **22**, 513.
2. Yang C. (2000) *Journal of Composite Materials* **34**(4), 332.
3. Whitney J., Nuismer R.J. (1974) *Journal of Composite Materials* **8**, 253.
4. Kleiber, M., Hien, T.D. (1992), *The stochastic finite element method, basic perturbation technique and computer implementation*. John Wiley & Sons, Chichester.
5. Bolotin, V.V. (1985) *Engineering Fracture Mechanics* **22**(3), 387.
6. *ANSYS User's Manual v. 5.5* (1999) ANSYS, Inc. Southpointe 275 Technology Drive Canonsburg.
7. Zweben, C. (1989) In: Delaware Composites Design Encyclopedia – Vol. 1, pp.49-72, Zweben, C., Hahn, H.T., Chou, T.-W. (Eds.). Technomic Publ., Lancaster.
8. Kinloch, A.J. (1987) *Adhesion and adhesives: science and technology*, Chapman & Hall.